Smooth-particle applied mechanics: Conservation of angular momentum with tensile stability and velocity averaging

Wm. G. Hoover
Department of Applied Science, University of California at Davis/Livermore and Lawrence Livermore National Laboratory, Livermore, California 94551-7808, USA

Carol G. Hoover
Methods Development Group, Department of Mechanical Engineering and Lawrence Livermore National Laboratory, Livermore, California 94551-7808, USA

Elizabeth C. Merritt
Department of Applied Science, University of California at Davis/Livermore, Livermore, California 94551-7808, USA
(Received 23 September 2003; published 30 January 2004)

Smooth-particle applied mechanics (SPAM) provides several approaches to approximate solutions of the continuum equations for both fluids and solids. Though many of the usual formulations conserve mass, (linear) momentum, and energy, the angular momentum is typically *not* conserved by SPAM. A second difficulty with the usual formulations is that *tensile* stress states often exhibit an exponentially fast high-frequency short-wavelength instability, ''tensile instability.'' We discuss these twin defects of SPAM and illustrate them for a rotating elastic body. We formulate ways to conserve angular momentum while at the same time delaying the symptoms of tensile instability for many sound-traversal times. These ideas should prove useful in more general situations.

DOI: 10.1103/PhysRevE.69.016702 PACS number(s): 02.70.Ns, 62.20.−x

I. INTRODUCTION

Isolated systems of particles which interact with ''central'' forces, such as the forces derived from pair potentials, conserve the total angular momentum of the system L. Keeping in mind that the fundamental forces in nature are pairwise-additive Coulomb forces, it is not surprising that this same conservation principle is obeyed by macroscopic samples of ''real materials'' too. To demonstrate conservation of angular momentum for the simplest sufficiently general model system case, consider a two-dimensional system composed of N mutually interacting similar particles of mass m. Assume that the potential energy is a sum of pair terms $\phi(r)$ depending only the distance of separation, r. The total (counterclockwise) angular momentum of such a system is given by a sum of all the particle contributions:

$$L \equiv \sum_i m[(xv_y)_i - (yv_x)_i] = \sum_i m(r^2\dot{\theta})_i = \sum_i m(rv_\theta)_i .$$

Here x and y and $r^2 = x^2 + y^2$ are all measured from the center of mass of the system.

Let us define the coordinate separations $x_{ij} = x_i - x_j$ and $y_{ij} = y_i - y_j$ for all those *pairs* of particles which are close enough to interact through the pair potential $\phi(r)$. Then, differentiation of the angular momentum with respect to time gives

$$\dot{L} = \sum_i \sum_j [x_i(yF/r)_{ij} - y_i(xF/r)_{ij}]$$

$$= \sum_{i<j} [x_{ij}(yF/r)_{ij} - y_{ij}(xF/r)_{ij}] \equiv 0,$$

confirming the familiar result (subject to the central-force assumption) that angular momentum is conserved. Here F is the scalar magnitude of the force, $F = -d\phi/dr$.

In continuum mechanics angular momentum in a medium subject to internal stresses evolves in a similar way. Changes in overall angular momentum only occur through torques exerted by external forces. The total angular momentum in a continuum becomes an integral over the volume (area in the two-dimensional cases we emphasize here),

$$L = \int dx \int dy \rho(xv_y - yv_x),$$

where the mass density ρ as well as the velocity $v = (v_x, v_y)$ depend continuously upon the spatial (x,y) coordinates. The velocities respond to the stress tensor σ (assumed to be symmetric, in order to avoid infinite angular acceleration rates for small elements of the continuum) through the equation of motion

$$\rho\dot{v} = \nabla \cdot \sigma.$$

In the present work we consider two-dimensional solids with an elastic stress tensor

$$\sigma \equiv \lambda(\nabla \cdot u)I + \eta[\nabla u + \nabla u^t].$$

where the two Lamé elastic constants λ and η are equal. For small stresses this continuum model corresponds exactly to a macroscopic $(N \to \infty)$ description of an elastically isotropic microscopic system of point masses interacting with central forces. In the continuum stress tensor I is the unit tensor and u is the vector displacement from the stress-free configuration. ∇u^t is the transpose of ∇u. We choose the two-

dimensional situation throughout this work in order to simplify the description. All of the ideas which we explore are equally valid and useful for more general constitutive relations and in three space dimensions.

In the discussion that follows we focus on a *particle* method for solving the *continuum* equations of motion, smooth-particle applied mechanics (SPAM). This classic method was developed, simultaneously and independently, by Lucy and by Monaghan, in 1977 [1,2]. We begin by sketching the structure of the method in Sec. II. Though the typical formulations of SPAM *do* conserve mass, (linear) momentum, and energy, they *do not* conserve *angular* momentum [3,4]. In Sec. III we analyze momentum conservation in continuum mechanics and show how the lack of conservation using SPAM can be expressed as a sum of short-ranged particle pair terms. The simplest formulation of SPAM is subject to a fast-growing "tensile instability" [5,6]. In Sec. IV we show that this instability can be avoided, for relatively long times, by simple algorithms based on the physical concepts of velocity averaging [7,8] and von Neumann's artificial viscosity [9]. To assess the usefulness of these approaches, we analyze the time development of plane waves, in Sec. V, as well as the steady rotation of an elastic body, in Sec. VI. The difficulties in solving the latter problem suggest a variety of ways to conserve angular momentum exactly while avoiding tensile instability. We develop and apply three methods to this problem in Secs. VII and VIII, pointing out in our conclusion (Sec. IX) that some of these methods can be successfully generalized to more complicated applications of SPAM.

We are well aware that many more-complicated particle methods have been, and are being, developed [10,11]. For the most part these more elaborate schemes rely on a spatial interpolation grid in addition to the grid defined by the particle positions themselves. Though some of these more complicated approaches can also cure the decays and instabilities we have studied here, we believe that the relative simplicity and efficiency of the simpler SPAM methods is better suited to large-scale numerical implementations.

II. SMOOTH-PARTICLE APPLIED MECHANICS

The smooth-particle method [1–16] for solving continuum problems is *not* consistent with the fundamental conservation principal for angular momentum. This is because the approach (unlike fundamental continuum mechanics) is *nonlocal* and the forces are not central. SPAM uses *extended* particles which typically exert torques on one another through shear stress. In fluids the shear stress is a consequence of Newtonian viscosity. In elastic solids the shear stress results from deformation. Just as in three dimensions a rotationally invariant shear stress magnitude can be defined in two dimensions as

$$\sigma^2_{\rm shear} \equiv \sigma^2_{xy} + \frac{1}{4}(\sigma^2_{xx} - \sigma^2_{yy}).$$

In any case smooth particles move according to motion equations with *noncentral* tensor forces involving the pressure tensors P (or stress tensors $\sigma \equiv -P$) for each ij pair of particles close enough to interact:

$$\left\{ \ddot{r}_i = \dot{v}_i = -m\sum_j \left[(P/\rho^2)_i + (P/\rho^2)_j \right] \cdot \nabla_i w_{ij} \right\}.$$

Although the "self" term, with $i=j$, is included in the sum it makes no contribution because the weight-function gradient vanishes for $r_{ij}=0$. Because the combination of antisymmetric terms, $\nabla_i w_{ij} + \nabla_j w_{ij}$, vanishes for $i \neq j$, it is evident that the summed-up linear momentum changes vanish, so that the overall linear momentum is conserved too. Likewise, the total smooth-particle energy $\Sigma m(e+v^2/2)$ is conserved. The time rates of change of the individual particles' internal energies $\{\dot{e}\}$ follow from the smooth-particle "energy equation"

$$\left\{ \dot{e}_i \equiv -\sum_j (m/2)\left[(P/\rho^2)_i + (P/\rho^2)_j \right] : (v_j - v_i) \nabla_i w_{ij} \right.$$
$$\left. - \sum_j m\left[(Q/\rho^2)_i + (Q/\rho^2)_j \right] \cdot \nabla_i w_{ij} \right\}.$$

The heat-flux Q contributions cancel in pairs while the work done by the pressure tensors $\{P\}$ exactly compensates the corresponding change in the kinetic energy $\dot{K} = \Sigma m v \cdot \dot{v}$. In all the smooth-particle equations w_{ij} is a normalized weight function with at least two continuous spatial derivatives and a finite range h. Lucy's quartic weight function is the simplest polynomial satisfying all these conditions:

$$w(r<h) = \frac{5}{\pi h^2}\left(1 - \frac{r}{h}\right)^3 \left(1 + 3\frac{r}{h}\right) \rightarrow \int_0^h 2\pi r dr w(r) \equiv 1.$$

The range of w is usually chosen such that each particle interacts with 20 or 30 others. Density can be computed in either one of the two ways: (i) summing up weight functions,

$$\rho_i = \rho(r_i) = m\sum_j w(r_i - r_j) \equiv m\sum w_{ij},$$

or (ii) integrating the sum's time derivative, so as to solve the smooth-particle analog of the continuity equation

$$\dot{\rho}_i = m\sum_j (v_i - v_j) \cdot \nabla_i w_{ij}.$$

In the summed-up form the maximum contribution to the density comes from the self-term $m w_{ii}(r_{ii}=0)$. The two methods are identical, provided that the initial densities for the continuity equation used in (ii) are chosen to match the summed-up values used in (i). The continuity formulation is more useful for systems which maintain well-defined surfaces.

Because the elastic displacements $\{u\}$ and their corresponding strains have no unambiguous meaning in particle simulations it is necessary to relate the stresses back to an initial condition. The time development of the stresses can

then be evaluated by solving the corresponding differential equations involving the velocity gradients $\nabla v=(d/dt)\nabla u$:

$$\dot{\sigma}\equiv\lambda(\nabla\cdot v)I+\eta[\nabla v+\nabla v^t],$$

supplemented by the additional changes resulting from coordinate rotations

$$\dot{\sigma}_{xx}\rightarrow\dot{\sigma}_{xx}-2\omega\sigma_{xy},\quad \dot{\sigma}_{yy}\rightarrow\dot{\sigma}_{yy}+2\omega\sigma_{xy},$$

$$\dot{\sigma}_{xy}\rightarrow\dot{\sigma}_{xy}+\omega(\sigma_{xx}-\sigma_{yy}),$$

where the local counterclockwise angular velocity ω is given by

$$\omega\equiv\frac{1}{2}\left(\frac{\partial v_y}{\partial x}-\frac{\partial v_x}{\partial y}\right).$$

The coordinate-rotation corrections follow naturally from the rigid-body rotation, at the angular frequency $\omega=\frac{1}{2}[(\partial v_y/\partial x)-(\partial v_x/\partial y)]$:

$$\sigma_{xy}=+\cos(2\omega t),\quad \sigma_{xx}=-\sin(2\omega t),\quad \sigma_{yy}=+\sin(2\omega t).$$

These differential equations, for $\{\dot{\sigma}_{xx},\dot{\sigma}_{xy},\dot{\sigma}_{yy}\}$, along with those for $\{\dot{\rho},\dot{x},\dot{y},\dot{v}_x,\dot{v}_y,\dot{e}\}$ can all be solved conveniently and accurately with fourth-order Runge-Kutta integration. If accuracy is not so important as speed, a lower-order integrator can be used.

III. TIME RATE OF CHANGE FOR ANGULAR MOMENTUM

A. $\dot{L}$ using SPAM

Substitution of the smooth-particle equations of motion for $\{\dot{v}=\dot{v}(\sigma,\rho,w)\}$ into the *particle* representation of $\dot{L}$ gives a (spurious) time rate of change for the angular momentum:

$$\dot{L}=\frac{d}{dt}m\sum\ (x\dot{y}-y\dot{x})$$

$$=m\sum\ (x\ddot{y}-y\ddot{x})$$

$$=\sum\ \dot{L}_{ij}$$

$$=m\sum_{ij}\ (x_{ij}y_{ij})\left[\left(\frac{P_{xx}}{\rho^2}\right)_i+\left(\frac{P_{xx}}{\rho^2}\right)_j-\left(\frac{P_{yy}}{\rho^2}\right)_i-\left(\frac{P_{yy}}{\rho^2}\right)_j\right]$$

$$\times(w'/r)_{ij}-m\sum_{ij}\ (x_{ij}^2-y_{ij}^2)\left[\left(\frac{P_{xy}}{\rho^2}\right)_i+\left(\frac{P_{xy}}{\rho^2}\right)_j\right]$$

$$\times(w'/r)_{ij}.$$

Generally there is no reason to expect this sum to vanish. Numerical evaluation confirms that $\dot{L}$ is typically nonzero.

Notice the close resemblance to the expression of the polar-coordinate shear stress $\sigma_{r\theta}$ in terms of the Cartesian-coordinate stress tensor:

$$\sigma_{r\theta}=-(\sigma_{xx}-\sigma_{yy})\sin(2\theta)+\sigma_{xy}\cos(2\theta)$$

$$=\frac{-xy}{r^2}(\sigma_{xx}-\sigma_{yy})+\frac{x^2-y^2}{r^2}\sigma_{xy}.$$

Consider a small element of ''surface'' (actually a length in two dimensions), $rd\theta$. The corresponding applied torque $dT=r\sigma_{r\theta}rd\theta$ differs from the shear stress $\sigma_{r\theta}$ on the surface element by the factor $r^2d\theta$.

Numerical investigation of isolated (torque-free) rotating bodies shows that the pairwise-additive smooth-particle contributions to the internal torque sum

$$T=\sum\ T_{ij}=\sum\ \dot{L}_{ij}\equiv\dot{L}$$

can be either positive or negative, with roughly equal numbers of each. There is an overall tendency, in the simple problems we studied, toward decay, with $\dot{L}/L$ negative, in the short term. At long times the angular momentum computed with SPAM fluctuates about zero. Evidently it is very desirable to improve SPAM so as to avoid this spurious behavior. Before implementing this improvement it is useful to compare the $\dot{L}$ expression from SPAM with $\dot{L}$ from conventional continuum mechanics.

B. $\dot{L}$ from continuum mechanics

A straightforward approach to calculating $\dot{L}$ in continuum mechanics can be based on the spatially averaged rate of change of the angular momentum, in a small $d\times d$ region with the sides of the region parallel to the x and y axes. To do so it is convenient to expand the stress divergence $\nabla\cdot\sigma$ as a Taylor's series about the center (of mass) of the region. The value at the region's center makes no net contribution. When the nonvanishing linear terms are accumulated the expression for $\dot{L}_{d\times d}$ becomes

$$\dot{L}_{d\times d}=\rho d^2\langle\delta x\,\delta\ddot{y}-\delta y\,\delta\ddot{x}\rangle$$

$$=d^2\left\langle\left[\delta x\left(\frac{\partial^2\sigma_{xy}}{\partial x^2}\right)\delta x-\delta y\left(\frac{\partial^2\sigma_{xy}}{\partial y^2}\right)\delta y\right]\right\rangle$$

$$=\frac{d^4}{12}\left[\frac{\partial^2\sigma_{xy}}{\partial x^2}-\frac{\partial^2\sigma_{xy}}{\partial y^2}\right].$$

Here $-d/2<\delta x,\ \delta y<+d/2$ are coordinates relative to the $d\times d$ square's center. From the physical standpoint this expression should be equivalent to a sum of the net torques exerted by surrounding material on the four faces ($\pm d/2$, $\pm d/2$). It is possible to confirm this correspondence in detail, by carrying out Taylor's series expansion of σ_{xy} including quadratic terms (the constant and linear terms all cancel), though we do not reproduce the details here. If the orienta-

tion of the small $d\times d$ region were rotated through an angle $\pi/4$, an alternative expression would result:

$$\dot{L}_{d\times d}=\frac{d^4}{12}\left[\frac{\partial^2(\sigma_{xx}-\sigma_{yy})}{\partial x\,\partial y}\right].$$

The smooth-particle expression for $\dot{L}$ of Sec. III A is essentially the rotationally invariant combination of the two results for $\dot{L}_{d\times d}$. In SPAM we expect that the length d would approximate the range h of the smooth-particle weight function so that the stress derivatives could just as well be approximated by an appropriate sum:

$$\dot{L}_i=m\sum_j\,(w/r^2)_{ij}[(xy)_{ij}(\sigma^\Sigma_{xx}-\sigma^\Sigma_{yy})-(x^2-y^2)_{ij}\sigma^\Sigma_{xy}],$$

where we use the notation σ^Σ to indicate *sums* of the i and j components. σ^Σ_{xx} indicates the sum of xx stress components for particles i and j, for instance. Another way to express the angular momentum as a sum of single-particle torque contributions $T_i=\dot{L}_i$ is to define $\dot{L}=\Sigma\dot{L}_i$, where $\dot{L}_i\equiv\frac{1}{2}\Sigma_{j\neq i}\dot{L}_{ij}$, using the SPAM $\{\dot{L}_{ij}=T_{ij}\}$ discussed in Sec. III A.

IV. TENSILE INSTABILITY FOR SPAM

Swegle, Hicks, and Attaway [5] displayed clear examples of a smooth-particle ''tensile instability.'' Ever since, that instability has been used to criticize the method. Swegle, Hicks, and Attaway found that neighboring smooth particles tend to clump together, exponentially fast at first, when the local stress is tensile rather than compressive. It is easy to see how this arises: if the stress and density are both slowly varying in space, then the smooth-particle equation of motion resembles a particle motion equation from ordinary Newtonian mechanics,

$$\dot{v}_i\equiv m\sum_j\,[(\sigma/\rho^2)_i+(\sigma/\rho^2)_j]\cdot\nabla_i w_{ij}\propto\sum_j\,-\nabla_i w_{ij}\,.$$

A *compressive* stress, with σ negative, corresponds to ordinary molecular dynamics, with $w(r)$ playing the role of a smooth repulsive potential. A *tensile* stress, with σ positive, corresponds to a purely attractive potential, and is an unstable situation.

Figure 1 shows the development of the tensile instability for a moving particle at the center of an otherwise motionless hexagonal sample. The velocity increases, exponentially fast, for five orders of magnitude. This unphysical instability needs to be tamed in order for SPAM to be applied to problems with tensile stresses. Any mechanism which prevents particles from approaching one another, or which substantially slows their approach, will do. For example, additional repulsive forces [6], an analog of von Neumann's artificial viscosity [1,9], a velocity-dependent central force, or velocity averaging [7,8], all of which can cause approaching particles to slow, are possibilities for taming the instability. We found that elastically reflecting the radial component of velocity for approaching pairs of particles, $v_r\equiv v_{ij}r_{ij}/|r_{ij}|$, at a fixed closest-approach distance, works quite nicely for this purpose and requires nothing more than a simple test. Velocity averaging appeals to us because it has also the effect of producing smoother flow fields than does standard SPAM. The short-time exponential tensile instability disappears completely if the smooth-particle equation relating the coordinates to the velocities, $\dot{r}_i\equiv v_i$, is replaced by a velocity equation using the *averaged* velocity at location r_i:

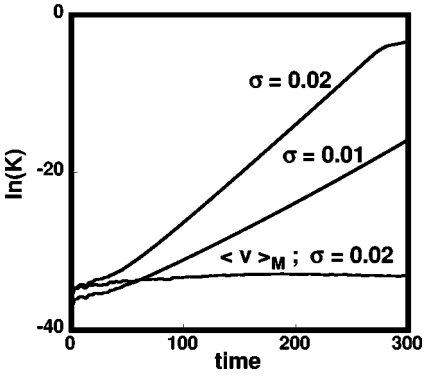

FIG. 1. Time development of the total kinetic energy in a many-body system in which a single particle is given a small initial velocity, 10^{-10}. Initially the remaining particles make up a motionless triangular lattice under uniform tension. The kinetic energy using the ''usual'' SPAM algorithm, which incorporates no velocity averaging and no artificial viscosity, with initial hydrostatic stresses $(\sigma_{xx}+\sigma_{yy})/2$ of 0.01 and 0.02, shows the stress-dependent exponential growth characteristic of tensile instability. Velocity averaging, with $\dot{r}=\langle v\rangle_{\rm Monaghan}$ and an initial stress of 0.02 shows no such instability for the time interval shown. The lattice ''collision time'' is of order unity.

$$\dot{r}_i\equiv\langle v\rangle;\quad \langle v\rangle\equiv\sum_j\,v_j w_{ij}\Big/\sum_j\,w_{ij}=\frac{m}{\rho_i}\sum_j\,v_j w_{ij}\,.$$

Note that the term with $i=j$ is typically the largest one in the sum. An alternative slightly more-complicated form is Monaghan's velocity-averaging equation

$$\dot{r}_i\equiv\langle v\rangle_{\rm Monaghan},\quad \langle v\rangle_{\rm Monaghan}\equiv v_i+\sum\,[v_j-v_i]\frac{w_{ij}}{\rho_{ij}},$$

$$\rho_{ij}\equiv\frac{1}{2}(\rho_i+\rho_j)\quad\text{or}\quad\sqrt{\rho_i\rho_j}.$$

Figure 1 shows clearly that the unstable exponential growth of kinetic energy associated with tension in standard SPAM disappears when Monaghan's velocity averaging is used. We will see that the extra complexity of Monaghan's approach is compensated by improved stability in problems involving tension. Either of the two averaging forms has the effect of *decreasing* the relative velocities of approaching (or receding) particles while exactly conserving linear momentum. The tensile instability is not a problem for long-wavelength disturbances. The short-ranged nature of the instability can be studied by analyzing the oscillation of plane waves, as we describe in the following section.

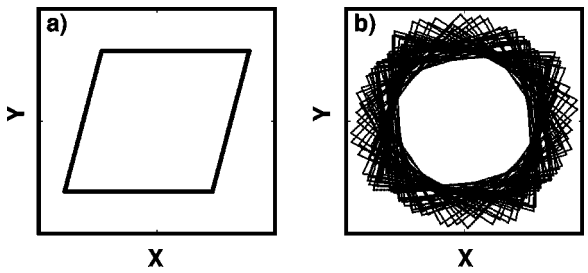

FIG. 2. Deformation of the unit square with the simple shear $u_x = y/4$. If the deformed configuration (a) is taken as a constraint-free initial condition the resulting motion oscillates symmetrically (b) and without any rotation about the center of mass.

V. ELASTIC PLANE-WAVE TEST PROBLEMS

One might imagine studying the oscillation of angular momentum in a deformed square, as is shown in Fig. 2, but a little reflection shows that the square undergoes purely vibrational oscillations, without any angular momentum. One of the horizontal boundaries of the square could be explicitly constrained in order to exert a torque, but a simpler implicit boundary-free problem results if instead we consider a standing plane shear wave, with wave vector $(k_x, k_y) \equiv (0, 2\pi/\lambda)$ parallel to the y direction. In such a wave the local angular momentum density varies periodically in space and time. Let the amplitude of oscillation be A_x with the initial condition such that the kinetic energy vanishes. The x displacement in this motion has the following form:

$$u_x(y,t) = A_x \sin(ky)\cos(\omega t).$$

The corresponding elastic strain $\epsilon_{xy} = \partial u_x/\partial y + \partial u_y/\partial x$ gives the only nonvanishing stress component $\sigma_{xy} \equiv \eta \epsilon_{xy}$. This stress component must satisfy the continuum equation of motion, $\rho \dot{v} \equiv \nabla \cdot \sigma$. The solution consistent with our assumed initial condition (specified in terms of the local stress) is

$$\epsilon_{xy} = kA_x \cos(ky)\cos(\omega t) \rightarrow \sigma_{xy} = \eta k A_x \cos(ky)\cos(\omega t),$$

$$\dot{x} = -\omega A_x \sin(ky)\sin(\omega t) \rightarrow \ddot{x} = -\omega^2 A_x \sin(ky)\cos(\omega t).$$

The stress and acceleration satisfy the usual continuum motion equation

$$\rho \ddot{x} = \frac{\partial \sigma_{xy}}{\partial y} = -\eta k^2 A_x \sin(ky)\cos(\omega t)$$

$$= -\rho \omega^2 A_x \sin(ky)\cos(\omega t),$$

which gives the familiar dispersion relation for the transverse sound speed $c_T = \omega/k = \sqrt{\eta/\rho}$. An exactly similar argument, but for a displacement in the y direction, leads to a solution of the corresponding motion equation and gives the corresponding dispersion relation for longitudinal waves:

$$u_y(y,t) = A_y \sin(ky)\cos(\omega t) \rightarrow c_L = \omega/k = \sqrt{\frac{\lambda + 2\eta}{\rho}}.$$

For Hooke's law harmonic forces, with force constant κ in a two-dimensional triangular lattice (with six nearest-neighbor interactions for each particle), the Lamé constants λ and η are equal (to $\sqrt{3/16}\kappa$) so that the longitudinal wave speed exceeds the transverse wave speed by $\sqrt{3}$.

The angular momentum in the transverse wave, averaged over all space, is zero, but the *local* angular momentum density

$$l = -\rho y \dot{x} = +\omega \rho A_x y \sin(ky)\sin(\omega t)$$

oscillates in space and time. Just as in Sec. III B, we consider the angular momentum contained within a small $d \times d$ region which moves with the flow velocity. In a $(\delta x, \delta y)$ system of coordinates, fixed on the center of mass of the region and comoving with it, the corresponding velocity $(\delta v_x, \delta v_y)$ varies linearly. The first-order term (in δy) then follows from the Taylor's series for v_x:

$$\delta v_x = \delta y \frac{\partial v_x}{\partial y} = k \delta y v_x,$$

so that the angular momentum of the $d \times d$ region is proportional to the mean value of δy^2 throughout the region. Its time derivative varies as $\cos(ky)\cos(\omega t)$:

$$\dot{L}_{d\times d} = \dot{l} d^2 = \rho d^2 \langle -\delta y \ddot{x} \rangle = \rho d^2 \omega^2 k \frac{d^2}{12} A_x \cos(ky)\cos(\omega t).$$

The time-rate-of-change can alternatively be calculated directly from the equation of motion for the small $d \times d$ square:

$$\rho d^2 \frac{d}{dt} \langle -\delta y \, \delta \dot{x} \rangle = \rho d^2 \langle -\delta y \, \delta \ddot{x} \rangle$$

$$= \rho d^2 \left\langle -\delta y^2 \frac{\partial \delta \ddot{x}}{\partial y} \right\rangle$$

$$= \rho d^2 \left\langle -\frac{\delta y^2}{\rho} \frac{\partial^2 \sigma_{xy}}{\partial y^2} \right\rangle$$

$$= \frac{d^4 \eta k^3}{12} A_x \cos(ky)\cos(\omega t).$$

That the two expressions for $\dot{L}$ must agree again implies the exact dispersion relation $c_T = \omega/k = \sqrt{\eta/\rho}$.

Both the angular momentum and its rate of change vanish as the *square* of the volume element's size. This problem is an excellent test for smooth-particle methods. Using a periodic crystal, 24 in width and $24\sqrt{3/4}$ in height, described by 576 particles at a mass density of $\sqrt{4/3}$, leads to a near-perfect periodic motion, with period 35. See Fig. 3 for two example problems, both with maximum displacements (in either the x or the y direction) equal to 0.25. For the transverse wave, with x displacements, the corresponding ω/k ratio closely approximates the transverse sound velocity $c_T = \sqrt{3/8}$:

$$\omega/k = (2\pi/35)/(2\pi/24\sqrt{3/4}) = 0.59 \simeq 0.61 = c_T.$$

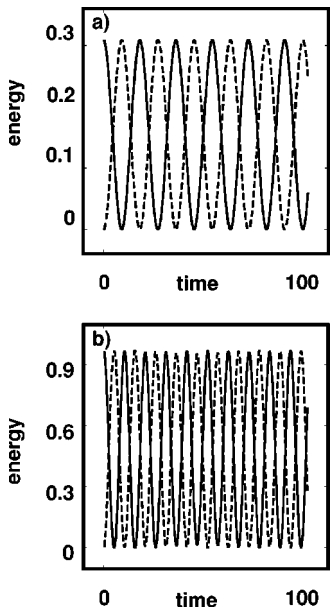

FIG. 3. Evolution of plane waves in a 24×24 sample of periodic linear elastic solid. The time variations of the kinetic (dashed) and internal (full curve) energies are shown. The initial condition is a sinusoidally deformed lattice, motionless, and with a sinusoidal distribution of the initial stresses. Both the transverse (a) and longitudinal (b) energies are shown. The oscillation frequencies agree with macroscopic linear elastic theory within about 1%.

The time dependence of the local angular momentum obeys the analysis given above.

A similar simulation, with $A_y=0.25$ rather than A_x, likewise reproduces the expected motion for *longitudinal* waves, with $c_L=\sqrt{9/8}$. See again Fig. 3. Evidently there is no problem with either tensile instability or with angular momentum conservation for these two simple test problems. We also confirmed that these solutions are stable to small random perturbations of the initial conditions. Let us turn next to a more challenging example.

VI. ROTATING TENSILE TEST PROBLEM

The stationary state of a rotating compressible *disk* is a standard problem in elasticity theory. In a rotating disk of radius R, density ρ, and with equal elastic constants $\lambda=\eta$ the (radial) displacement and nonvanishing stress-tensor components are

$$u_r=\frac{\rho r\omega^2}{6}\left(R^2-\frac{2r^2}{3}\right), \quad \sigma_{rr}=\frac{5\rho\omega^2}{12}(R^2-r^2),$$

$$\sigma_{\theta\theta}=\frac{5\rho\omega^2}{12}\left(R^2-\frac{3r^2}{5}\right).$$

Discrete particles suggest using a hexagonal sample shape. Detailed stress and displacement comparisons with molecular dynamics show only small deviations between the circular and hexagonal sample shapes.

With SPAM, the stability of a *rotating* compressible solid is quite different to molecular dynamics and to the plane-wave motions of the preceding section. Figure 4 shows snapshots of the motion of three 217-particle elastic solids with equal Lamé constants. At the top we see a standard molecular dynamics simulation, using fourth-order Runge-Kutta integration with a nearest-neighbor pair potential $\phi=\frac{1}{2}(1-r)^2$ and a particle mass of unity has a stress-free density of $\sqrt{4/3}$ and two equal elastic constants $\eta=\lambda=\sqrt{3/16}$. In all cases, the initial velocities are chosen to correspond to rigid-body rotation, with a maximum speed (at the vertices of the hexagon) equal to 0.1. This maximum speed is a bit less than 10% of the longitudinal sound speed. This relatively slow motion guarantees sufficiently small strains (of order $0.1^2=0.01$) for the applicability of linear elasticity.

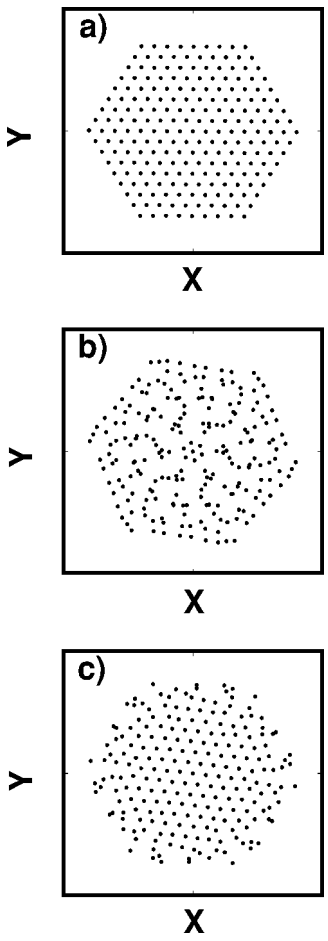

FIG. 4. Configurations of 217 particles after a nominal rotation of $2\pi/3$ using standard molecular dynamics (a), standard smooth-particle mechanics (b) with summed-up densities, and smooth-particle mechanics with densities based on the continuity equation (c) with initial values $\rho(t=0)\equiv\sqrt{4/3}$.

In the center of Fig. 4 we see the corresponding SPAM simulation, using Lucy's weight function with a range equal to three times the initial nearest-neighbor separation. Here we use the simple summation approach to density, $\rho\equiv m\Sigma w$. Below we integrate the continuity equation from the specified initial density $\rho=\sqrt{4/3}$. There are quite definite quantitative differences in the last two approaches, with the hexagonal lattice persisting better when the continuity equation is used. The summation approach has the advantage that

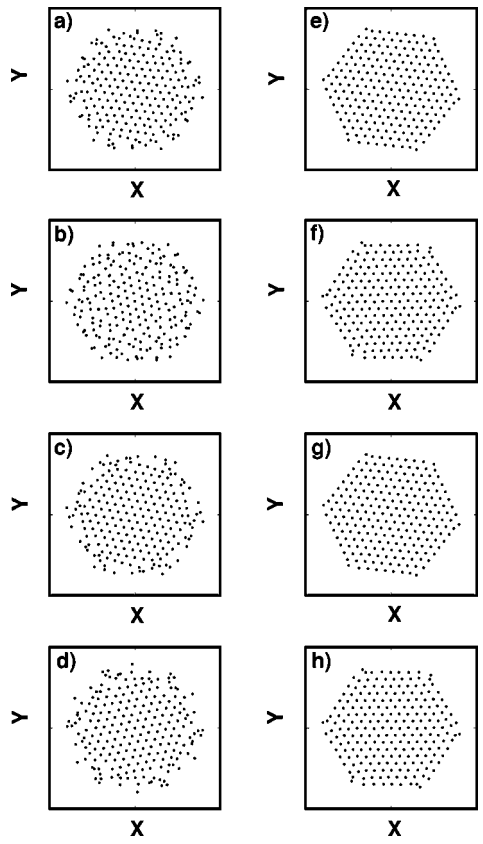

FIG. 5. Configurations of 217 particles after nominal rotations of $2\pi/3$ (top row) and 2π (second row) using SPAM with $\dot{r}\equiv\langle v\rangle$ (a,b) and SPAM with Monaghan's average $\dot{r}\equiv\langle v\rangle_{\text{Monaghan}}$ (e,f). The two types of average velocity are described in Sec. VI. Densities in these four simulations are all computed from the usual SPAM continuity equation with the initial value $\rho(t=0)\equiv\sqrt{4/3}$. Densities below, (c,d) and (g,h), for the same nominal rotations of $2\pi/3$ (third row) and 2π (fourth row) are computed using the chain-rule generalization of the continuity equation described at the end of Sec. VI. These examples clearly demonstrate the enhanced stability of Monaghan's velocity-averaging algorithm.

the total system mass obtained by integrating the mass density ρ is equal to Nm, where N is the number of particles and all the particle masses are the same, m. Nevertheless, in the remaining simulations we have used the continuity-equation approach, which generated ''better'' solutions from the shape-conserving standpoint.

The molecular dynamics algorithm provides stable solutions which conserve both energy and angular momentum as accurately as desired (up to the precision carried by the computer). The standard SPAM algorithm, with the same number of particles, the same elastic equation of state, and the same stress-free density, behaves qualitatively differently. It results in a loss of 1% (5%) percent of the angular momentum after a rotation of 60° (120°) degrees. Figure 5 (above) shows the improved motion which results when the particle velocities are replaced by the local averages described in Sec. IV. On the left we use the ordinary SPAM velocity average:

$$\{\dot{r}_i=v_i\}\rightarrow\left\{\dot{r}_i=\langle v\rangle\equiv\frac{m}{\rho_i}\sum_j v_j w_{ij}\right\},\quad \rho_i=m\sum w_{ij}.$$

Monaghan's slightly more complicated suggestion (which has the advantage of exactly conserving linear momentum) provides similar results (shown at the right of Fig. 5). Monaghan's form for the average is different:

$$\left\{\dot{r}_i=v_i+\sum_j (v_j-v_i)w_{ij}/\rho_{ij}\right\},$$

where the mean density ρ_{ij} can be either arithmetic or geometric:

$$\rho_{ij}=\frac{\rho_i+\rho_j}{2}\quad\text{or}\quad\rho_{ij}=\sqrt{\rho_i\rho_j}.$$

It should be pointed out (but has not been, so far as we know) that the *velocity-averaged* forms for $\dot{r}$ are inconsistent with the usual smooth-particle continuity and energy equations. We do not wish to carry out a full investigation here. A thorough investigation is certainly warranted. Here we have chosen to solve a few selected problems using continuity equations properly modified for velocity averaging:

$$\dot{\rho}_i\equiv m\sum_j\langle v_i-v_j\rangle\cdot\nabla_i w_{ij}$$

$$\text{or}\quad\dot{\rho}_i\equiv m\sum_j\langle v_i-v_j\rangle_{\text{Monaghan}}\cdot\nabla_i w_{ij}.$$

Results from both these approaches appear in the lower part of Fig. 5. The usual SPAM velocity average is used on the left and Monaghan's velocity average on the right.

Notice that it is possible to simulate the rotation fairly well for a complete rotation, a time of order 30 sound traversal times, when velocity averaging is used. Though the two velocity averaging ideas illustrated here, as well as several others, can be used to avoid the tensile instability, all the SPAM simulations, modified or not, suffer from a relatively rapid loss of angular momentum. We cure this loss in the following section.

VII. ANGULAR MOMENTUM CONSERVATION IN SPAM USING GAUSS'S PRINCIPLE

An overall correction could be constructed by adding a torque counteracting the change associated with each ij pair:

$$T_{ij}\propto\dot{L}_{ij}=m(x_{ij}y_{ij})\left[\left(\frac{P_{xx}}{\rho^2}\right)_i+\left(\frac{P_{xx}}{\rho^2}\right)_j-\left(\frac{P_{yy}}{\rho^2}\right)_i-\left(\frac{P_{yy}}{\rho^2}\right)_j\right]$$

$$\times(w'/r)_{ij}-m(x_{ij}^2-y_{ij}^2)\left[\left(\frac{P_{xy}}{\rho^2}\right)_i+\left(\frac{P_{xy}}{\rho^2}\right)_j\right](w'/r)_{ij}.$$

This correction violates conservation of energy to the extent that the rotational kinetic energies are changed; and it is not at all clear that sufficient radial kinetic energy is available to correct for this violation. Furthermore, more complicated situations cannot be simply treated in this way. A good example is a system composed of *two* specimens, identical ex-

cept for the direction of rotation, clockwise for one and counterclockwise for the other. Evidently the equations of motion conserve angular momentum exactly for such a system despite the exactly compensating losses in the two specimens.

Except in certain special cases SPAM does not conserve angular momentum. In smooth-particle mechanics it is desirable to conserve the angular momentum *without* disturbing energy conservation. Consider imposing the energy and angular momentum constraints simultaneously,

$$\dot{E}=0=\sum m(\dot{e}+v\cdot\dot{v}), \quad \dot{L}=0=\sum m(x\ddot{y}-y\ddot{x})$$

by using the generalized equations of motion

$$\{m\dot{v}=F_{\mathrm{SPAM}}+\mathcal{F}\}.$$

Here the constraint force $\mathcal{F}$ keeps both the energy and the angular momentum fixed. Out of all the possible constraint forces Gauss' principle [15,16] (of least constraint) can be used to pick the smallest (in an rms sense). The result identifies two multipliers α, which constrains the energy E, and β, which constrains the angular momentum L. The equations of motion which result are

$$\mathcal{F}_x=-\alpha\dot{x}-\beta y, \quad \mathcal{F}_y=-\alpha\dot{y}+\beta x;$$

$$\alpha=-\beta L/(2K), \quad \beta=\dot{L}/[mR^2-(mL^2/2K)].$$

Here $R^2=\Sigma r^2$ is the moment of inertia about the center of mass. The denominator $[R^2-(L^2/2K)]$ vanishes for a pure rigid-body motion, for which the constraints are unnecessary. Unfortunately the same denominator vanishes periodically in the more general case, so that this constraint method is not generally useful. The physical significance of the multipliers is clear: the Lagrange multiplier α controls the kinetic energy through a generalized frictional force (which can either add or subtract energy); the Lagrange multiplier β controls the angular momentum by exerting torques on every particle. The singular divergence of the multipliers occurs when there is insufficient radial kinetic energy to compensate for the work of keeping the angular momentum constant. In the following section we describe an alternative approach which does not suffer from the singular behavior of the two Gauss' principle multipliers.

VIII. ANGULAR MOMENTUM CONSERVATION IN SPAM USING TORQUE SCALING

We carried out a wide range of simulations to test the various ideas for stabilizing a rotating body. Here we report some sample results for hexagonal specimens with a maximum rotational velocity of 0.1 (where the nearest-neighbor triangular-lattice spacing is unity and the transverse and longitudinal sound velocities are, respectively, $\sqrt{3/8}$ and $\sqrt{9/8}$). We reduced the variety of possible algorithms by choosing to omit von Neumann's artificial viscosity and to use Lucy's weight function, with a range three times the nearest-neighbor spacing $h\equiv 3$. Regular hexagons, with a maximum

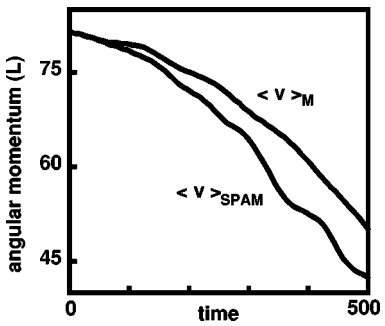

FIG. 6. Angular momentum as a function of time for the 217 particles shown in Fig. 5 using SPAM with velocity averaging, with $\dot{r}\equiv\langle v\rangle$ and with Monaghan's velocity average, $\dot{r}\equiv\langle v\rangle_{\mathrm{Monaghan}}$. All densities here are from the continuity equation, corresponding to the top two rows of Fig. 5.

center-to-perimeter distance n in the stress-free state, and $N=7,19,37,61,\ldots=1+3n+3n^2$ particles with initial tangential particle velocities $r\dot{\theta}=0.1r/n$ were followed for the time $20n\pi$, which would correspond to a complete rotation (and several sound-traversal times). For illustrative purposes we use the case $n=8\rightarrow N=217$ in the figures.

Standard SPAM, due to the tensile instability, is unable to retain the hexagonal sample shape for long. Whether the initial density is chosen everywhere equal to the ideal stress-free triangular-lattice density $\rho=\sqrt{4/3}=1.1547$ (and updated by integrating the $\dot{\rho}$ continuity equation) or is instead evaluated by approximate smooth-particle summing $\rho_i\equiv\Sigma_j w_{ij}$, where 1.1551 is the approximate perfect-lattice density, the resulting simulation is still poor. Either of these approaches satisfies the smooth-particle continuity equation

$$\dot{\rho}=-\rho\nabla\cdot v\leftrightarrow\dot{\rho}_i\equiv m\sum_j (v_i-v_j)\cdot\nabla_i w(r_{ij}).$$

Though the hexagonal sample shape survives fairly well for a complete revolution, the angular momentum is decreased to about half its initial value. See Fig. 6. In the absence of constraint forces angular momentum decays relatively promptly. Velocity averaging cures the tensile instability, at least for a few sound-traversal times, but does not help with angular momentum conservation. In curing the angular momentum loss, as described below, we retain velocity averaging in order to stave off tensile instability too.

Gauss' principle suggests that angular momentum be conserved by adding an additional force proportional to each particle's distance from the center of mass. We reject that idea in favor of local corrections which do not depend upon the global coordinates. To get a local formulation consider the time rates of change $\{\dot{L}_{ij}\}$ of the angular momenta associated with all interacting pairs of particles:

$$\dot{L}=\frac{d}{dt}m\sum (x\dot{y}-y\dot{x})=\sum_{ij}\dot{L}_{ij},$$

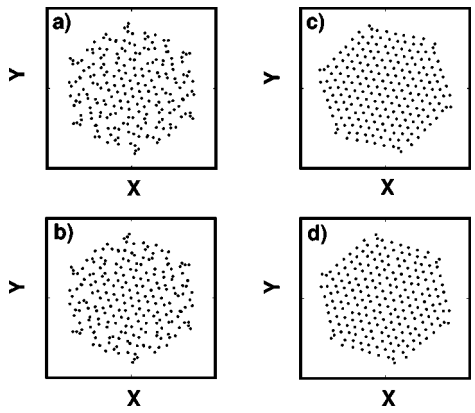

FIG. 7. Configurations of 217 particles, with angular momentum held fixed, after nominal rotations of 2π. SPAM using $\dot{L}_{ij}$ torque scaling appears at the top and with $\dot{L}_i$ scaling at the bottom. $\dot{r} \equiv \langle v \rangle$ (a,b) and SPAM with Monaghan's average, $\dot{r} \equiv \langle v \rangle_{\text{Monaghan}}$ (c,d) are shown. The two types of average velocity are described in Sec. VI. Summed-up densities $\rho_i = m\Sigma_j w_{ij}$ perform much less well than do the continuity-equation densities used in all these simulations.

$$\dot{L}_{ij} \equiv (x_{ij}y_{ij})\left[\left(\frac{P_{xx}}{\rho^2}\right)_i + \left(\frac{P_{xx}}{\rho^2}\right)_j - \left(\frac{P_{yy}}{\rho^2}\right)_i - \left(\frac{P_{yy}}{\rho^2}\right)_j\right](w'/r)_{ij}$$

$$-(x_{ij}^2 - y_{ij}^2)\left[\left(\frac{P_{xy}}{\rho^2}\right)_i + \left(\frac{P_{xy}}{\rho^2}\right)_j\right](w'/r)_{ij}.$$

One can equally well define individual particle time rates of change in terms of sums of the $\dot{L}_{ij}$:

$$\dot{L}_i = \frac{1}{2}\sum_j \dot{L}_{ij}.$$

In a typical SPAM simulation several thousands of $\dot{L}_{ij}$ are negative. The rest are positive, and the sum is nearly zero. The sum could be made to be *exactly* zero by rescaling the negative and positive $\dot{L}_{ij}$:

$$\dot{L}_{ij} < 0 \rightarrow R^{+1}\dot{L}_{ij}, \quad \dot{L}_{ij} > 0 \rightarrow R^{-1}\dot{L}_{ij},$$

where R^2 is the sum of all the positive $\dot{L}_{ij}$ divided by minus the sum of the negative $\dot{L}_{ij}$. In an exactly similar way $\{\dot{L}_i\}$ can also be scaled so as to vanish exactly. These two ideas provide definite improvements over the usual SPAM algorithm. Snapshots taken after a full revolution at fixed angular momentum and with both kinds of velocity averaging are shown in Fig. 7.

IX. SUMMARY AND CONCLUSIONS

An exhaustive exploration of smooth-particle algorithms is a daunting task. The literature includes *many* versions of the equations of motion and many definitions for smooth-particle gradients. We have consistently used what seem to us to be the *simplest* definitions throughout:

$$\dot{v}_i \equiv \sum_j [(\sigma/\rho^2)_i + (\sigma/\rho^2)_j] \cdot \nabla_i w(r_{ij}),$$

$$(\nabla v)_i \equiv \sum_j (v_{ij}/\rho_{ij}) \nabla_i w(r_{ij}), \quad v_{ij} \equiv v_i - v_j,$$

$$\rho_{ij} \equiv (\rho_i + \rho_j)/2.$$

Nevertheless, many variations and combinations are possible: (i) restricting the distance of closest approach, or not; (ii) using von Neumann's viscosity, or not; (iii) computing density as a sum or by integrating the continuity equation; (iv) advancing the coordinates with

$$\dot{r} = v \quad \text{or} \quad \langle v \rangle \quad \text{or} \quad \langle v \rangle_{\text{Monaghan}};$$

(v) constraining the angular momentum with Gauss' principle, with $\{T_i = \dot{L}_i\}$, or with $\{T_{ij} = \dot{L}_{ij}\}$. Just these $2 \times 2 \times 2 \times 3 \times 3 = 72$ combinations, most of which we have explored, could be expanded to include weight functions $w(r < h)$ other than Lucy's, and with ranges other than $h = 3$, as well as less accurate but more efficient time integrators. An even greater variety of algorithms can be generated by following the consequences of velocity averaging, as we indicated at the end of Sec. VI. We have made an effort to specify precisely here what we have done in order that others could reproduce our results without excessive difficulty.

We have seen that the combination of Monaghan's velocity averaging with a conservative local constraint on the angular momentum provides good solutions of a rotating body under tensile stress conditions and for many sound-traversal times. In a more general situation, such as the fragmentation of a bar by a projectile, *local* conservation of angular momentum is necessary. To see that the locality of the constraint is essential, consider a system composed of two mirror-image counter rotating hexagons. One rotates clockwise while its twin rotates counterclockwise. No matter how poorly angular momentum is conserved locally, the global sum vanishes. Any general treatment requires dividing the system into parts, each of which must satisfy its own angular momentum balance. With this separation into parts there is no problem rescaling the positive and negative $\{\dot{L}_{ij}\}$ or $\{\dot{L}_i\}$ for each part, resulting in both local and global conservation.

Under compressive loads the various smooth-particle methods have no special drawbacks. In general, one cannot expect smooth particles to perform well using the present methods in *quasistatic* tensile simulations. The present work demonstrates that velocity averaging (or viscosity, or a minimum distance of closest approach) can provide accurate simulations for times on the order of 20 sound-traversal times.

ACKNOWLEDGMENTS

W.G.H.'s work in Carol Hoover's Methods Development Group at the Lawrence Livermore National Laboratory was performed under the auspices of the United States Depart-

ment of Energy through University of California Contract No. W-7405-Eng-48. E.C.M.'s work at the Department of Applied Science was supported by a research grant from the Academy of Applied Science (Concord, New Hampshire). Both Timur Ismagilov and Jeffrey Marchese (Department of Applied Science, Livermore) provided some useful comments in the course of this work, as did also Harald Posch (Wien) and Oyeon Kum (Clemson).

[1] J.J. Monaghan, Annu. Rev. Astron. Astrophys. **30**, 543 (1992).
[2] L. Lucy, Astron. J. **82**, 1013 (1977).
[3] J. Bonet and T.S.L. Lok, Comput. Methods Appl. Mech. Eng. **180**, 97 (1999).
[4] S. Nugent and H.A. Posch, Phys. Rev. E **62**, 4968 (2000).
[5] J.W. Swegle, D.L. Hicks, and S.W. Attaway, J. Comput. Phys. **116**, 123 (1995).
[6] J.J. Monaghan, J. Comput. Phys. **82**, 290 (2000).
[7] J.J. Monaghan, J. Comput. Phys. **82**, 1 (1989).
[8] J.P. Gray, J.J. Monaghan, and R.P. Swift, Comput. Methods Appl. Mech. Eng. **190**, 6641 (2001).
[9] F. Vesely, *Computational Physics, an Introduction* (Plenum, New York, 1994), Sec. 8.1.3.
[10] T. Belytschko, Y. Guo, W.K. Liu, and S.P. Xiao, Int. J. Numer. Methods Eng. **48**, 1359 (2000).
[11] A.K. Chaniotis, D. Poulikakos, and P. Koumoutsakos, J. Comput. Phys. **82**, 67 (2002).
[12] Wm.G. Hoover and C.G. Hoover, Comput. Sci. Eng. **3**, 78 (2001).
[13] O. Kum, Wm.G. Hoover, and H.A. Posch, Phys. Rev. E **52**, 4899 (1995).
[14] Wm.G. Hoover, H.A. Posch, V.M. Castillo, and C.G. Hoover, J. Stat. Phys. **100**, 313 (2000).
[15] Wm. G. Hoover, *Time Reversibility, Computer Simulation, and Chaos* (World Scientific, Singapore, 1999).
[16] W. G. Hoover, *Computational Statistical Mechanics* (Elsevier, New York, 1991).